Cell shape anisotropy enhances cytoplasm viscoelastic resistance to stabilize mitotic spindle position during early embryo development

Jing Xie [1,2,3,4], Javad Najafi [1,2] , Luc Lederer [1,2] , Aude Nommick [1,2], Jeremy Salle [1,2] , Serge Dmitrieff [1,2], and Nicolas Minc [1,2,#]

[1] Université Paris Cité, CNRS, Institut Jacques Monod, F-75013 Paris, France

[2] Equipe Labellisée LIGUE Contre le Cancer

[3] Current address : Institut Curie, PSL Research University, CNRS UMR144, Laboratoire Biologie Cellulaire et Cancer, 75005 Paris, France.

[4] Current address : Institut Curie, PSL Research University, Sorbonne Universite, CNRS UMR3664, Laboratoire Dynamique du Noyau, 75005 Paris, France.

Corresponding author: NM: nicolas.minc@ijm.fr

Author Contributions: Conceptualization, N.M., J.X. and J.N.; Methodology, N.M., S.D., J.S., A.N., L.L, J.N. and J.X. Writing –Original Draft, N.M., J.X. and J.N. Draft Editing. N.M., S.D., J.S., A.N., L.L, J.N. and J.X.

Competing Interest Statement: The authors declare no competing interest.

Classification: BIOLOGICAL SCIENCES; Cell Biology; PHYSICAL SCIENCES; Biophysics and Computational Biology

Keywords: Cell division; Embryogenesis, Mitotic spindles; Forces; Cytoplasm; Flows; Rheology

ABSTRACT:

Cell geometry is an important element in the regulation of mitotic spindle positioning during early embryo development and tissue morphogenesis. To date, however, we still lack an understanding for how intracellular forces that position and stabilize mitotic spindles depend on cell geometry. Here, we used *in vivo* magnetic tweezers to directly measure the forces that maintain the mitotic spindle in the center of sea urchin blastomeres that change sizes and shapes during early embryo development. We found that spindles are held by viscoelastic forces that progressively increase in amplitude at subsequent developmental stages, as cells become smaller and also more elongated in shape. Using simulations, cell shape manipulations and cytoplasm flow analysis, we attribute these mechanical changes to an enhancement of cytoplasm viscoelastic resistance that emerges from stronger hydrodynamic coupling between the spindle and cellular boundaries as cell shapes become more anisotropic. Therefore, this study suggests a novel shape-sensing system for division positioning mediated by cytoplasm hydrodynamics with functional implications for early embryo morphogenesis.

Significance Statement

The regulation of mitotic spindle positioning is a key process for tissue architecture, embryo development and stem cells. In many embryos and tissues, cell shape has been proposed to influence the force balance that positions mitotic spindles during cell division. However, direct measurement of the impact of cell geometry on spindle positioning forces are still lacking. Here, using magnetic tweezers to directly measure forces that hold spindles in the cell center, throughout early embryo development, we evidence a direct scaling between cell shape anisotropy and spindle positioning forces. Our data support a model in which the primary effect of cell geometry is to impact the hydrodynamic coupling between the spindle and cell boundaries mediated by the cytoplasm fluid.

INTRODUCTION

Cell division is critical to promote the multicellularity of developing embryos and tissues. Cells usually divide at precise locations and along precise axes, a process often crucial for tissue morphogenesis and cell fate decisions (1–3). The position of the division plane is specified by the mitotic spindle, a large microtubule-based assembly that resides in the cytoplasm. Spindles can rotate or translate during mitosis to eventually adopt a final stable position that they maintain to specify cleavage furrow assembly (4–6). Force-generating cytoskeletal networks such as microtubule asters and associated motors or acto-myosin contractile bundles are well-established regulators of both spindle movements and stability (7–11). These cytoskeleton elements connect the cell surface to spindle poles for force exertion. When cytoskeleton forces are imbalanced around cells, the spindle will translocate or rotate. When they are balanced, the spindle will hold its position and orientation. In addition to active force generators, the passive viscoelastic properties of bulk cytoplasm were also recently proposed to contribute to hold spindle in place, by opposing spindle displacement and springing it back to its initial position when perturbed (12). Therefore, spindle positioning may result from a complex integration of different active and passive mechanical inputs.

One challenge associated with the study of mitotic spindle positioning during development, is given by the large range of cell shapes and sizes found in developing embryos or tissues. For instance, as early embryos develop, dividing blastomeres can vary in size over 2-3 orders of magnitude. Moving or maintaining a spindle in the center of a large versus a small cell, may for instance require very different mechanisms (13, 14). Cell shapes can also vary extensively during development and has been shown to influence spindle positioning, with spindles that commonly align along the longest cell shape axis (15–20). In general, however, how mechanical elements that regulate spindle positioning may be adapted to the size or shape of cells during development to promote an accurate division remains unknown.

To address this question, we used *in vivo* magnetic tweezers to directly measure the forces that maintain mitotic spindles in the center of early dividing sea urchin blastomeres. We found that spindles are held by viscoelastic forces that progressively increase in strength from the 1- to the 2 and the 4-cell stages, as blastomeres become smaller and also more anisotropic in shape. By manipulating cell shape, we demonstrate that cell shape anisotropy is sufficient to increase the

amplitude of spindle positioning forces. Using finite-element hydrodynamics simulations and cytoplasm flow analysis, we propose that cell shape anisotropy enhances cytoplasm viscoelastic resistance on spindles, as a result of stronger hydrodynamic interactions between the spindle and cell boundaries.

RESULTS

Mitotic spindles are held by viscoelastic forces in the center of early blastomeres

Mitotic spindles are generally bounded in size by microtubule (MT) dynamic instabilities, to an upper limit of ~30-40 µm in length (21–23). As a consequence, in many large zygotes and early blastomeres that exceed this size threshold, spindles are prepositioned by cell-spanning interphase asters and then hold their positions in the cell center without contacting the cell cortex (15, 24). We recently proposed that the cytoplasm holds these spindles in the center of large sea urchin zygotes that are ~95µm in diameter, by opposing spindle displacement with viscoelastic reactive forces (12). We sought to explore the relevance of this regime throughout early embryogenesis when cells become smaller as a result of rounds of reductive divisions (Movie S1). Using immunostaining to label MTs, F-actin and DNA, and airy-scan confocal microscopy, we computed the distance between MT +TIPs to the actin-rich cortex in metaphase from the 1- to the 16-cell stage (Fig. 1A and Fig. S1A-B). The mean distance was 14.48 +/- 2.65 µm (+/-SD) in zygotes, and gradually reduced at subsequent stages to reach a distance of 2.54 +/- 2.34 µm at the 16-cell stage (Fig. 1B and Fig. S1C). These distances represented a relatively stable fraction of ~15% of cell length from the 1 to the 4-cell stage, but sharply transited to only ~6 % from the 8-cell stage onward (Fig 1C and Fig. S1D). These analyses suggest that spindles are uncoupled from the cell surface up to the 4-cell stage in this system, and rather float in bulk cytoplasm.

To assay the type and magnitude of forces that hold spindles in the center of early blastomeres we applied calibrated forces on mitotic spindles along the spindle axis in zygotes, 2- and 4-cell blastomeres using *in vivo* magnetic tweezers (Movie S2 and Fig. 1D-G). These assays rely on the injection of specific magnetic beads that recruit dynein to self-target themselves to the centrosomes, and form compact aggregates that stay attached to centrosomes throughout early embryo development (12, 25, 26). Interestingly, the displacement-time curves for the motion of

spindles under external magnetic forces exhibited similar behavior from the 1 to the 4-cell stage, indicative of similar mechanisms holding spindles in the cell center. First, the spindle moved at constant speed following a viscous regime, and then slowed down indicating the presence of internal elastic forces that oppose spindle displacement. On longer time-scales, the spindle recovered a constant speed suggesting a progressive fluidization of elastic elements (Fig. 1H). In agreement with the existence of an elastic response, when the force was released, spindles recoiled back towards the cell center. However, this recovery was only partial, with spindles recoiling only ~50% of the distance moved under force. This indicates significant dissipation of stored elastic energy (Fig. S1F). Importantly, at all developmental stages, both rising and relaxation responses were well-fitted by a Jeffreys' 3-element fluid model, that was previously used to model bulk cytoplasm viscoelasticity (12, 27, 28). These results suggest that spindles from the 1- to the 4-cell stages are held in the cell center by viscoelastic spring-like forces from bulk cytoplasm.

Fitting rising curves with Jeffreys' model allowed us to compute a restoring stiffness for the spindle as well as a viscous drag. Interestingly, the restoring stiffness increased gradually from the 1- to the 4-cell stages, with values of 55.34+/-28.8, 68.41+/-28.21 and 79.75+/-20.03 pN/µm (+/-SD), respectively. Therefore, spindle restoring stiffness increased by 24% at the 2-cell stage and 44% at the 4-cell stage, as compared to the zygote stage (Fig. 1I). Viscous drags also increased by 52% at the 2-cell stage and 29% at the 4-cell stage (Fig. S1G). As a result of both simultaneous increase in restoring stiffness and drags, viscoelastic time-scales remained at similar values independent of developmental stages, in agreement with spindle recoils occurring at the same rates (Fig. S1F and S1H). These results indicate that the effective viscoelastic resistance of bulk cytoplasm on mitotic spindles may increase in strength during early embryo development.

Hydrodynamic simulations suggest that cell shape anisotropy may enhance cytoplasm viscoelastic resistance on spindles

We hypothesized that such an increase in viscoelastic resisting forces could result from 3 potential non-mutually exclusive effects: an alteration of cytoplasm physical properties, a decrease in cell size, or a change in cell shape. Indeed, as embryos develop, blastomeres halve

their volume at each division cycle, but also change shape significantly, transiting from a round zygote to two hemispherical 2-cell blastomeres and to four ellipsoidal 4-cell blastomeres. To begin challenging these hypotheses, we implemented finite-element simulations to model the response of a spindle moved by external forces in a viscoelastic fluid enclosed in different geometries (28). The spindle was modeled as a rigid impermeable ellipsoidal object with dimensions taken from experimental measurements at different developmental stages (Fig. S2A). Cell shapes and sizes were obtained by cutting the 1-cell sphere into two hemispheres for the 2-cell stage and into four quarters for the 4-cell stage (Fig. 2A and Table S1). The cytoplasm was implemented as a viscoelastic fluid using an Oldroyd-B model, which is equivalent to the Jeffreys' model used to analyze experimental curves (28). Importantly, the cytoplasm fluid was assumed to obey no-slip conditions at the interface with both spindle and cell boundaries. To simulate magnetic pulls on spindles, a constant step force was applied to one half of the ellipsoid (the spindle) using a boundary load. At the beginning of each simulation, the spindle was placed in the center of mass of the geometry which coincides with the origin of the coordinate system, and also aligned with the longest shape axis, as in experiments. We simulated both pulling and relaxation, and fitted the displacement-time curve of the spindle to compute simulated values of drags and restoring stiffnesses.

To isolate the effect of cell size, we first ran simulations in spheres of reducing volumes and scaled the spindle according to experimental measurements, but kept all other parameters identical (Fig 2I and Table S1). These simulations did not predict any systematic increase in restoring stiffness as observed in experiments, presumably because spindles scale with cell size during early sea urchin embryogenesis (23), and because simulations are mostly insensitive to absolute size values. We next simulated spindle response by inputting both cell shape and size variations as in experiments (Fig 2B and Movie S3). Remarkably, these simulations predicted that changes in cell shapes can lead to a progressive increase in both spindle restoring stiffnesses and drags similar to experimental behavior (Fig. 2C, Fig. 2I and, Fig. S2C). By inspecting the viscoelastic flows generated along the spindle in simulations, we observed that this increase appeared to be associated with the proximity of cell boundaries to the spindle, that may limit cytoplasm backflows and therefore increase viscoelastic resistance (Fig 2C and Movie S3). Theses simulation results suggest that an anisotropic cell shape may enhance the effective cytoplasm viscoelastic resistance on spindles.

To test if cytoplasm physical properties could also evolve and influence resistance to spindle movement, we injected small 1µm beads in the cytoplasm of 1-, 2- or 4-cell blastomeres in metaphase, and displaced them in between spindles and the cell surface with calibrated magnetic tweezers (Fig 2D-E). Single bead displacement under force curves were also inflected, reflecting the viscoelastic properties of bulk cytoplasm (27) (Fig 2F). By fitting displacement-time curves with a Jeffreys' model, we computed values for cytoplasm stiffness and viscosity. However, as beads were moved in between spindles and the cell surface, we corrected these values to account for a confinement between two planes, using a measured vertical distance between spindles and the cell cortex (Fig S2B). This analysis revealed a minor increase in both cytoplasm stiffness and viscosity at the scale of these small objects (Fig 2G-H). However, as cytoplasm rheology was proposed to be scale-dependent (28–30), we assayed how inputting these different cytoplasm viscoelastic constants into the hydrodynamics model affected spindle behavior under force. We found that predicted spindle restoring stiffnesses were much higher than in experiments (Fig 2I). These simulation results suggest that the slight increase in the cytoplasm viscoelasticity measured at a 1µm scale may not simply explain the progressive enhancement of resistance on spindles with developmental stages.

Manipulation of cell shape is sufficient to alter cytoplasm viscoelastic resistance on spindles

To more directly test the predicted contribution of cell shape anisotropy to the amplitude of viscoelastic forces that hold mitotic spindles in the cell center, we designed experiments to manipulate cell shapes and compute these forces with magnetic tweezers. We first experimentally rounded 2-cell stage blastomeres using a transient treatment with Calcium-free sea water, that disrupts cell-cell adhesion. This caused blastomeres to round within few minutes, without affecting cell volume, metaphase duration or spindle size (Fig 3A-B and Fig S3A-C). By applying magnetic pulls to mitotic spindles in these round 2-cell stage blastomeres (Fig 3C and Movie S4), we found a reduction of both spindle restoring stiffness and viscous drag by 0.83X and 0.67X, respectively, as compared to those of control elongated blastomeres (Fig. 3D-E and Fig. S3D). Accordingly, simulations performed using the geometry of these rounded 2-cell blastomeres also predicted a reduction in both stiffness and drag, as compared to elongated

controls (Fig. 3F and Fig. S3F). These results indicate that a rounded cell geometry may alleviate cytoplasm viscoelastic resistance to facilitate spindle displacements.

Next, we sought to perform the converse experiments, and increase cell shape anisotropy and test impact on spindle positioning forces. Starting with round zygotes, we devised U-shaped microfabricated chambers of various dimensions made in SU-8 resin that protrude above a cover-glass allowing to alter cell geometry while applying magnetic forces with the tweezer system (Fig. 4A and Movie S5). Eggs were gently pushed into chambers using a glass needle, injected with magnetic beads, and then fertilized (Fig. S4A). To explore dose-dependent effects, we used two sets of chambers in which cells were pushed into elongated shapes of mean aspect ratio of 1.24 and 1.49, respectively (Fig. 4D-E). In chambers, metaphase spindles moved with external magnetic forces exhibited a displacement that reflected a viscoelastic behavior similar to control, and relaxed back to the cell center when the force was removed (Fig. 4B-C, 4F, Fig. S4E, and Movie S5). Interestingly, the measured restoring stiffness was significantly higher than in control round zygotes, increasing by 1.29X in the first set of chambers and by 1.57X in the more anisotropic chambers (Fig. 4G). Viscous drags also increased by 1.27X and 1.22X, respectively (Fig. S4D). By performing simulations using the 3D rectangular cuboid shape of eggs pushed in the two sets of chambers we predicted an increase of restoring stiffness of 1.57X and 1.58X in the two sets of chambers, and an increase in viscous drags of 1.31X and 1.30X (Fig. 4H and Fig. S4F-H). These results directly support a significant impact of cell shape anisotropy on the amplitude of viscoelastic forces that hold spindles in the cell center.

Cell shape anisotropy enhances the shear of cytoplasm viscoelastic flows when spindles are displaced.

To understand how cell shape may enhance the effective cytoplasm viscoelastic resistance on spindles, we mapped cytoplasm flows during spindle motion using Particle Image Velocimetry of large granules in cells (12, 28). In both control round zygotes and deformed ones in microchambers, flows exhibited two large vortices on the two sides of moving spindles, indicative of large cytoplasm fluid shear in between the cell and spindle boundaries (Fig. 4I-J). Interestingly, the size of vortices, measured as the width of the gradient in flow velocities, was much smaller in eggs deformed in chambers as compared to control round eggs, indicating a

much higher shear when cell shapes become more anisotropic (Fig. 4K and S5A). Accordingly, by simulating fluid flows caused by spindle movements in diverse cell geometries, we found that a confined geometry led to a dose-dependent decrease in the size of vortices and thus an increase in fluid shear with cell shape anisotropy (Fig. S5B-E). Finally, to generalize the influence of cell geometry on cytoplasm viscoelastic resistance on spindles, we ran a series of simulations in which we systematically altered cell geometry and computed spindle restoring stiffness and drags. This showed that the aspect ratio of the cell cross-section orthogonal to the spindle axis, may serve as a key parameter to predict viscoelastic enhancement, with higher aspect ratio that yield to increased viscoelastic resistance, in a dose-dependent manner (Fig. S5 F-H). We conclude that an important impact of cell shape on spindle positioning forces, may stand in the hydrodynamic coupling between the spindle and the cell surface, that increase when cells become more elongated and narrower.

DISCUSSION

The forces that position and orient mitotic spindles are fundamental elements to understand division plane positioning and consequent tissue morphogenesis. However, these forces have only been rarely measured (7, 12, 31), given the technical difficulties of directly attaching force probes on spindle poles in intact live cells. Here, we employed a magnetic tweezer set up to directly measure these forces in intact developing embryos, at multiple developmental stages. We found that mitotic spindles are held in the center of early blastomeres by large viscoelastic forces, that may reach several hundreds of pN, when spindles are offset by only few µm. These forces oppose spindle displacement and partially restore its initial position upon perturbation. Analysis of astral MTs length suggests that spindles lack direct contact with the surface, in early blastomeres up to the 4-cell stage. Together with signatures of spindle displacement under force, these data suggest that most of these forces may be attributed to bulk cytoplasm that act as a viscoelastic medium that holds spindles in the cell center (12). Importantly, we find that these re-centering viscoelastic forces increase in strength with developmental stages. Such increase may have functional implication for spindle stability, by maintaining a relative spindle centering precision mostly constant as cells become smaller during development (7, 14).

Using finite-element hydrodynamic simulations and cell shape manipulations we primarily attribute this mechanical enhancement to an increase in cell shape anisotropy as early blastomeres divide and change shape. When cells become more elongated, their cross-section around spindles becomes narrower, limiting space for the cytoplasm fluid to backflow around spindles, thereby enhancing viscoelastic resistance, much like in a piston (28, 32, 33). Therefore, a major output of our study is to put forward a new "cell shape sensing" mechanism based on the influence of cellular boundary on cytoplasm hydrodynamics with direct consequences on the mechanics of organelle positioning. As cell shape anisotropy typically increases during early cleavage in many embryos (34), we anticipate this regime to be highly relevant to the mechanics of spindle positioning in early dividing blastomeres. In addition, such an effect could also impact organelle positioning in highly elongated columnar epithelial cells that line embryo surfaces later in development. This hydrodynamics shape sensing mechanism may have important implication for mechanisms of spindle positioning. First, as directly demonstrated in our assay in which we force cells to adopt a rounded shape (Fig. 3), the net mechanical forces that hold spindles in the cell center are alleviated in rounded cells, suggesting that a rounded geometry may effectively facilitate spindle translation or rotation. As many somatic cells round up during mitosis (19, 35), such an effect could ease spindle rotation or asymmetric displacement needed for oriented or asymmetric divisions. Second, enhancing cytoplasm viscoelastic resistance in elongated cells, may help stabilize spindles in the cell center, when the cell's longest dimensions become too large for cytoskeletal based system to interact with the cell surface along this axis (36). In general, addressing how cytoplasm mechanics and fluid dynamics may intersect with cell geometry will bring important insights into questions of organelle positioning and tissue morphogenesis (37).

In addition to cell shape anisotropy, we also found that the cytoplasm may become slightly stiffer and more viscous when probed at a scale of 1 µm in successive early blastomeres (Fig. 2D-2H). Although we discarded such effect as being the main cause for the enhancement of viscoelastic resistance at the scale of large spindles, it raises fundamental questions on the regulation of cytoplasm crowding and mechanics during embryo development. Such progressive rigidification could result from alterations in the density or arrangements of cytoplasm crowders such as bulk actin networks, intermediate filaments, or endomembrane suspensions; or alternatively reflect changes in metabolic activity that agitate and fluidize the cytoplasm (38–40). Future *in vivo* force

measurements will reveal how bulk cytoplasm material properties may evolve during development to regulate multicellular morphogenesis.

ACKNOWLEDGMENT

We thank all members of the Minc team for discussion and technical help. J.X. acknowledges the "École Doctorale FIRE - Program Bettencourt", a fellowship from the Chinese Scholarship Council (201708070046) and from the labex "Who Am I". J.N. is supported by a Post-doc fellowship from the ARC foundation (PDF20191209818) and is an EMBO Non-Stipendiary Fellow (ALTF 881-2019). A.N. is supported by a Post-doc fellowship from the ARC foundation (PDF2021070004082). This work was supported by the Centre National de la Recherche Scientifique (CNRS), the Université de Paris, and grants from La Ligue Contre le Cancer (EL2021.LNCC/ NiM), the Agence Nationale pour la Recherche (ANR, "TiMecaDev"), the Fondation Bettencourt Schueller ("Coup d'élan"), a scientific subvention from the foundation "Simone and Cino Del Duca" and the European Research Council (ERC CoG "Forcaster" no. 647073 and ERC PoC "MagMech" No. 101069173) to N.M.

Material and methods

Detailed methods are provided in the SI appendix. They include protocols to obtain and handle sea urchin animals and gametes, and procedures used for live and fixed imaging of zygotes and early blastomeres. We also provide all detailed procedures for injecting magnetic beads, calibrating magnetic forces *in vitro*, and computing magnetic forces *in vivo*, as well as extracting viscoelastic parameters and mapping and analyzing viscoelastic flows in live cells. Finally, all details regarding hydrodynamic simulations are provided.

REFERENCES

1. J. Sallé, N. Minc, Cell division geometries as central organizers of early embryo development. *Semin Cell Dev Biol*, S1084-9521(21)00208–1 (2021).

2. B. G. Godard, C.-P. Heisenberg, Cell division and tissue mechanics. *Current Opinion in Cell Biology* **60**, 114–120 (2019).

3. T. Lechler, M. Mapelli, Spindle positioning and its impact on vertebrate tissue architecture and cell fate. *Nat Rev Mol Cell Biol* **22**, 691–708 (2021).

4. D. R. Burgess, F. Chang, Site selection for the cleavage furrow at cytokinesis. *Trends Cell Biol* **15**, 156–62 (2005).

5. E. V. van Leen, F. di Pietro, Y. Bellaïche, Oriented cell divisions in epithelia: from force generation to force anisotropy by tension, shape and vertices. *Current Opinion in Cell Biology* **62**, 9–16 (2020).

6. P. Gonczy, Mechanisms of asymmetric cell division: flies and worms pave the way. *Nat Rev Mol Cell Biol* **9**, 355–66 (2008).

7. C. Garzon-Coral, H. A. Fantana, J. Howard, A force-generating machinery maintains the spindle at the cell center during mitosis. *Science* **352**, 1124–7 (2016).

8. J. Azoury, *et al.*, Spindle positioning in mouse oocytes relies on a dynamic meshwork of actin filaments. *Curr Biol* **18**, 1514–9 (2008).

9. S. W. Grill, J. Howard, E. Schaffer, E. H. Stelzer, A. A. Hyman, The distribution of active force generators controls mitotic spindle position. *Science* **301**, 518–21 (2003).

10. A. Chaigne, *et al.*, F-actin mechanics control spindle centring in the mouse zygote. *Nat Commun* **7**, 10253 (2016).

11. J. Xie, N. Minc, Cytoskeleton Force Exertion in Bulk Cytoplasm. *Front. Cell Dev. Biol.* **8** (2020).

12. J. Xie, *et al.*, Contribution of cytoplasm viscoelastic properties to mitotic spindle positioning. *Proc Natl Acad Sci U S A* **119**, e2115593119 (2022).

13. T. Mitchison, *et al.*, Growth, interaction, and positioning of microtubule asters in extremely large vertebrate embryo cells. *Cytoskeleton (Hoboken)* **69**, 738–50 (2012).

14. J. Howard, C. Garzon-Coral, Physical Limits on the Precision of Mitotic Spindle Positioning by Microtubule Pushing forces: Mechanics of mitotic spindle positioning. *Bioessays* **39** (2017).

15. N. Minc, D. Burgess, F. Chang, Influence of Cell Geometry on Division-Plane Positioning. *Cell* **144**, 414–426 (2011).

16. A. Haupt, N. Minc, How cells sense their own shape - mechanisms to probe cell geometry and their implications in cellular organization and function. *J Cell Sci* **131** (2018).

17. M. Thery, M. Bornens, Cell shape and cell division. *Curr Opin Cell Biol* **18**, 648–57 (2006).

18. O. Hertwig, Ueber den Werth der ersten Furchungszellen fuer die Organbildung des Embryo. Experimentelle Studien am Frosch- und Tritonei. *Arch. mikr. Anat.* **xlii**, 662–807 (1893).

19. F. Bosveld, *et al.*, Epithelial tricellular junctions act as interphase cell shape sensors to orient mitosis. *Nature* **530**, 495–8 (2016).

20. R. Niwayama, *et al.*, A Tug-of-War between Cell Shape and Polarity Controls Division Orientation to Ensure Robust Patterning in the Mouse Blastocyst. *Developmental Cell* **51**, 564-574.e6 (2019).

21. E. M. Rieckhoff, *et al.*, Spindle Scaling Is Governed by Cell Boundary Regulation of Microtubule Nucleation. *Current Biology* **30**, 4973-4983.e10 (2020).

22. M. Wühr, *et al.*, Evidence for an Upper Limit to Mitotic Spindle Length. *Current Biology* **18**, 1256–1261 (2008).

23. B. Lacroix, *et al.*, Microtubule Dynamics Scale with Cell Size to Set Spindle Length and Assembly Timing. *Dev Cell* **45**, 496-511 e6 (2018).

24. M. Wuhr, E. S. Tan, S. K. Parker, H. W. Detrich, T. J. Mitchison, A model for cleavage plane determination in early amphibian and fish embryos. *Curr Biol* **20**, 2040–5 (2010).

25. J. Salle, *et al.*, Asymmetric division through a reduction of microtubule centering forces. *J Cell Biol* **218**, 771–782 (2019).

26. H. Tanimoto, J. Salle, L. Dodin, N. Minc, Physical Forces Determining the Persistency and Centering Precision of Microtubule Asters. *Nat Phys* **14**, 848–854 (2018).

27. Y. Hiramoto, Mechanical properties of the protoplasm of the sea urchin egg. I. Unfertilized egg. *Exp Cell Res* **56**, 201–8 (1969).

28. J. Najafi, S. Dmitrieff, N. Minc, Size- and position-dependent cytoplasm viscoelasticity through hydrodynamic interactions with the cell surface. *Proceedings of the National Academy of Sciences* **120**, e2216839120 (2023).

29. J. Hu, *et al.*, Size- and speed-dependent mechanical behavior in living mammalian cytoplasm. *Proc Natl Acad Sci U S A* **114**, 9529–9534 (2017).

30. B. R. Parry, *et al.*, The Bacterial Cytoplasm Has Glass-like Properties and Is Fluidized by Metabolic Activity. *Cell* **156**, 183–194 (2014).

31. M. I. Anjur-Dietrich, *et al.*, Clustering of cortical dynein regulates the mechanics of spindle orientation in human mitotic cells. 2023.09.11.557210 (2023).

32. J. Happel, H. Brenner, *Low Reynolds number hydrodynamics: with special applications to particulate media* (Springer Science & Business Media, 2012).

33. E. Nazockdast, A. Rahimian, D. Zorin, M. Shelley, A fast platform for simulating semi-flexible fiber suspensions applied to cell mechanics. *Journal of Computational Physics* **329**, 173–209 (2017).

34. S. F. Gilbert, *Developmental Biology. 9th edition.* (Sinauer Associates, 2010).

35. M. Thery, M. Bornens, Get round and stiff for mitosis. *HFSP J* **2**, 65–71 (2008).

36. J. Saleh, *et al.*, Length limitation of astral microtubules orients cell divisions in murine intestinal crypts. *Dev Cell* **58**, 1519-1533.e6 (2023).

37. A. Badugu, A. Käch, Cytoplasmic flows caused by actomyosin contraction drive interkinetic nuclear migration. 2020.04.09.034660 (2020).

38. M. Bonucci, T. Shu, L. J. Holt, How it feels in a cell. *Trends in Cell Biology* (2023) https:/doi.org/10.1016/j.tcb.2023.05.002 (June 13, 2023).

39. K. Luby-Phelps, Cytoarchitecture and physical properties of cytoplasm: volume, viscosity, diffusion, intracellular surface area. *Int Rev Cytol* **192**, 189–221 (2000).

40. M. I. Arjona, J. Najafi, N. Minc, Cytoplasm mechanics and cellular organization. *Current Opinion in Cell Biology* **85**, 102278 (2023).

FIGURES AND FIGURE LEGENDS

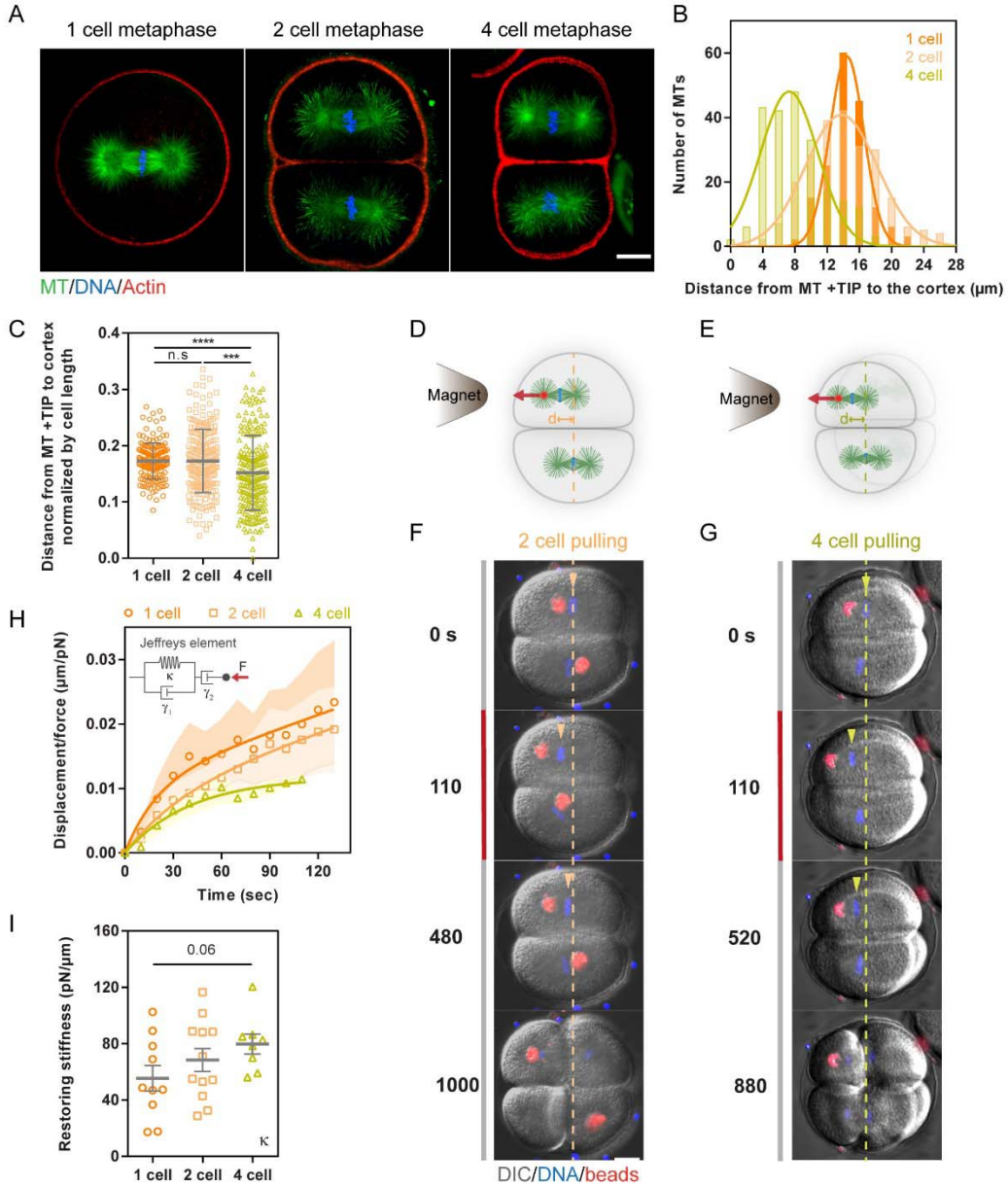

Figure 1. Mitotic spindles are held in the center of early blastomeres by cytoplasm viscoelastic forces that increase in strength with developmental stages. **(A)** Airy-scan confocal images of sea urchin embryos at 1-cell (left), 2-cell (middle) and 4-cell stage (right) in metaphase fixed and stained for Microtubules (MTs), DNA and F-actin. **(B)** Quantification of the distance from MT+ TIPS to the actin cortex in 1-cell, 2-cell and 4-cell stage embryos at metaphase (n= 168, 229 and 220 MTs from 4 independent embryos, respectively). **(C)** Quantification of the distance from MT+ TIPS to the actin cortex normalized by cell length for the same cells and conditions as in B). **(D-G)** Schemes and time-lapses of metaphase spindles in 2-cell stage (D and F) and 4-cell stage (E and G) with magnetic beads bound to one spindle pole, displaced by magnetic forces applied parallel to the spindle axis from the presence of a magnet tip (red line), and recoiling upon force cessation. Dotted lines correspond to the initial centered position of the spindle and arrow heads indicate the position of chromosomes. **(H)** Time evolution of the displacement measured from the initial centered position of the spindle normalized by the applied magnetic force for metaphase spindles in 1-cell, 2-cell and 4-cell embryos (n=10,12 and 8 cells respectively). The bold lines correspond to fits of the data using a Jeffreys' viscoelastic model (see main text and methods). Error bars are represented as shades in these curves correspond to +/- SD/2. **(I)** Cytoplasm restoring stiffness on mitotic spindles moved parallel to the spindle axis for the same cells and conditions as in H, computed using fits to the Jeffreys' models (n=10,12 and 8 cells respectively). Error bars correspond to +/- SEM. Results were compared by using a two-tailed Mann–Whitney test, and P-values are reported on the graph. Scale bars, 20 µm.

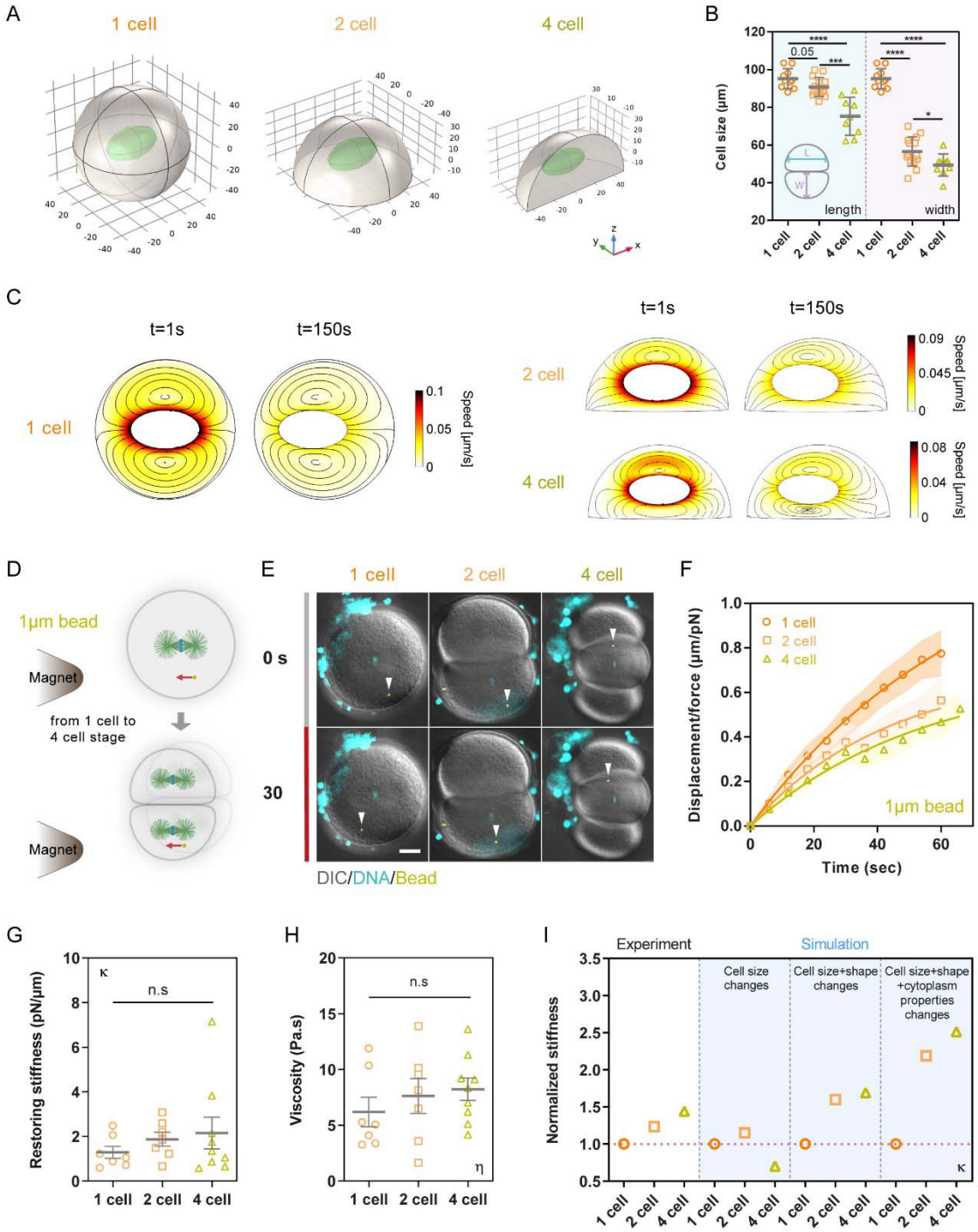
A
1 cell
2 cell
4 cell
B
Cell size (µm)
0.05
length
width
1 cell
2 cell
4 cell
C
t=1s
t=150s
1 cell
2 cell
4 cell
Speed [µm/s]
D
1µm bead
Magnet
from 1 cell to
4 cell stage
Magnet
E
1 cell
2 cell
4 cell
0 s
30
DIC/DNA/Bead
F
Displacement/force (µm/pN)
1 cell
2 cell
4 cell
1µm bead
Time (sec)
G
Restoring stiffness (pN/µm)
κ
n.s
1 cell
2 cell
4 cell
H
Viscosity (Pa.s)
n.s
η
1 cell
2 cell
4 cell
I
Experiment
Simulation
Cell size changes
Cell size+shape changes
Cell size+shape +cytoplasm properties changes
Normalized stiffness
κ
1 cell
2 cell
4 cell

Figure 2. Hydrodynamic simulation to model the impact of cell size, shape and cytoplasm properties on spindle restoring stiffness. (A) Schematic of cell and spindle geometries at different developmental stages taken to simulate the response of spindles to applied forces in a viscoelastic cytoplasm. **(B)** Cell dimensions of 1-, 2- and 4-cell stages blastomeres. **(C)** Stream lines and fluid flow speeds corresponding to 2 time-points (beginning and end of pulling) of hydrodynamic simulations of spindles moving under force in a viscoelastic medium confined by cell boundaries. **(D)** Scheme representing injected 1µm magnetic bead displaced with magnetic tweezers in the metaphase cytoplasm from the 1-cell to the 4-cell stage. **(E)** Time-lapses of injected 1 µm magnetic beads displaced by magnetic forces (red line) in the metaphase cytoplasm from 1-cell stage to 4-cell stage. White arrow heads point at the 1 µm bead position. **(F)** Time evolution of the displacement measured from the initial position of the 1µm bead normalized by the applied magnetic force in the metaphase cytoplasm of 1-cell, 2-cell and 4-cell embryos (n=8, 7 and 9 respectively). Error bars are represented as shades in these curves and correspond to +/- S.D/2. **(G-H)** Quantification of cytoplasm restoring stiffness κ and viscosity η for the same cells and conditions as in F, computed using fits to the Jeffreys' models. Error bars correspond to +/- SEM. **(I)** Restoring stiffness normalized by the 1-cell stage value compared between data from experiments and different sets of simulation considering changes in cell size only, in cell size and shape, and in cell size, shape and cytoplasm properties. The red dotted line corresponds to a value of 1. Results were compared by using a two-tailed Mann–Whitney test. n.s, $P > 0.05$, *, $P < 0.05$. Scale bars, 20 µm.

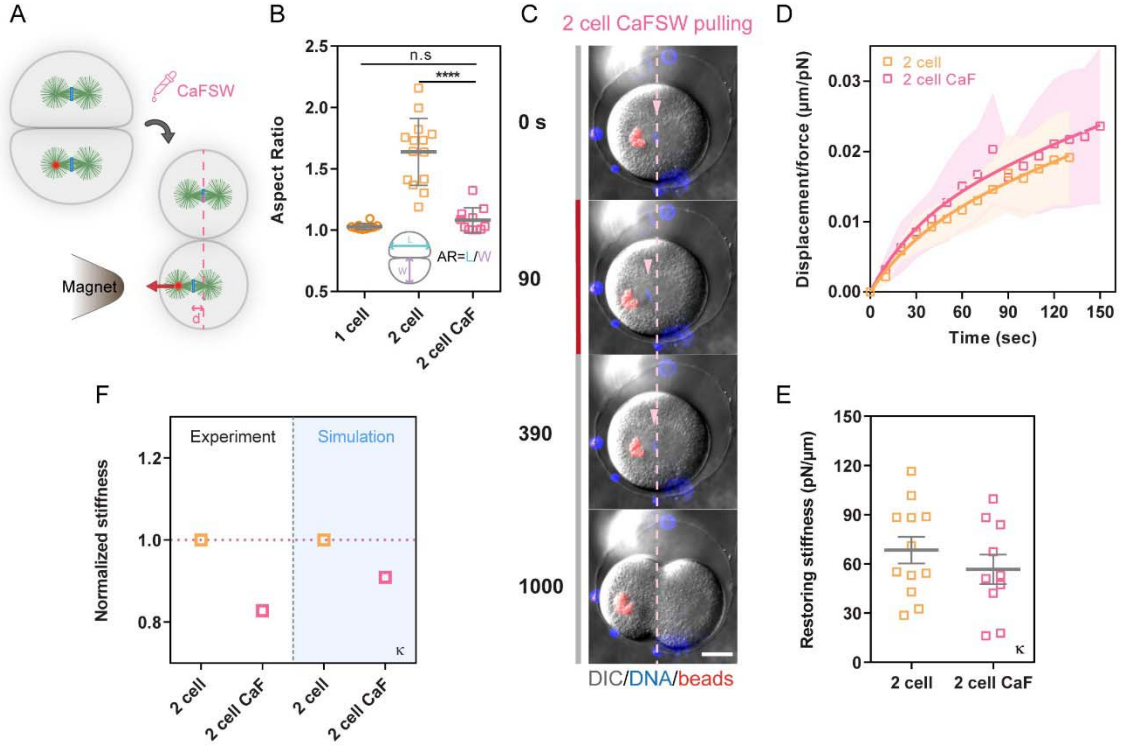
A
CaFSW
Magnet
B
Aspect Ratio
n.s
****
AR=L/W
1 cell
2 cell
2 cell CaF
C
2 cell CaFSW pulling
0 s
90
390
1000
DIC/DNA/beads
D
Displacement/force (μm/pN)
2 cell
2 cell CaF
Time (sec)
E
Restoring stiffness (pN/μm)
2 cell
2 cell CaF
F
Normalized stiffness
Experiment
Simulation
2 cell
2 cell CaF
2 cell
2 cell CaF

Figure 3. A rounded cell shape alleviates cytoplasm viscoelastic resistance on spindles. (A) Schemes of metaphase spindles in 2-cell stage blastomeres treated with CaFSW, to round up cell shapes with magnetic beads bound to one spindle poles. **(B)** Aspect ratios measured as indicated in the inset for cells in different conditions or stages (n=10,14 and 11 cells respectively). (C) Time-lapse of spindles in 2-cell stages blastomeres treated with CaFSW to round cell shapes, displaced by magnetic forces applied parallel to the spindle axis from the presence of a magnet tip (red line), and recoiling upon force cessation. Dotted lines correspond to the initial centered position of the spindle and arrowheads indicate the position of chromosomes. **(D)** Time evolution of the displacement of metaphase spindles at 2-cell stage normalized by the applied force for controls and cells treated with CaFSW (n=12 and 10 cells respectively). Error bars are represented as shades in these curves and correspond to +/- SD/2. **(E)** Cytoplasm restoring stiffness on mitotic spindles for the same cells and conditions as in D (n=12 and 10 cells respectively). Error bars correspond to +/- SEM. **(F)** Restoring stiffness normalized by the 2-cell control value in indicated conditions for experimental data vs simulations. Results were compared by using a two-tailed Mann–Whitney test. The corresponding P-values are indicated in the plot. Scale bars, 20 µm. Error bars correspond to +/- SD unless otherwise indicated.

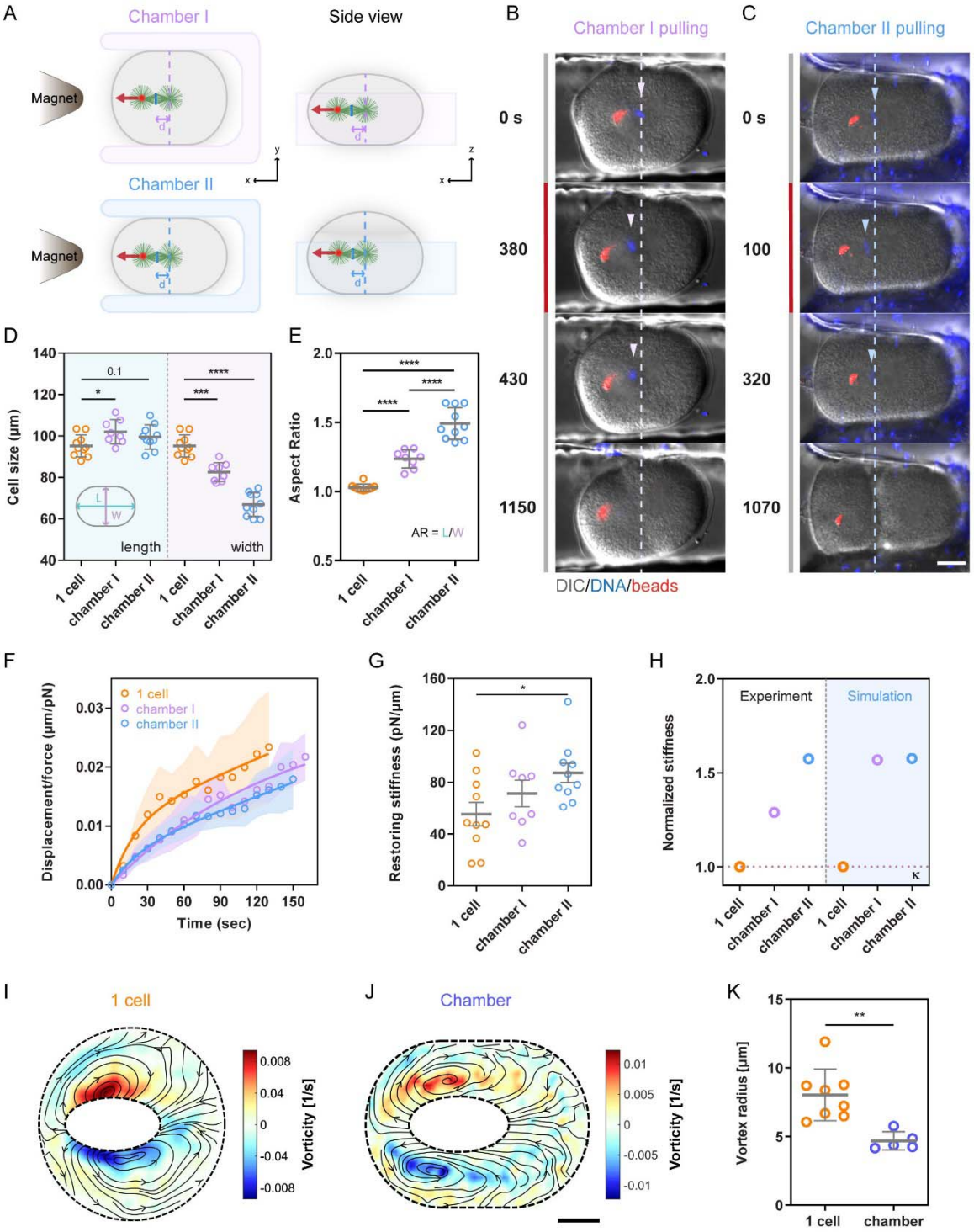
A
Chamber I
Side view
Magnet
Chamber II
Magnet
B
Chamber I pulling
0 s
380
430
1150
C
Chamber II pulling
0 s
100
320
1070
DIC/DNA/beads
D
Cell size (µm)
0.1
*
***
****
length
width
1 cell
chamber I
chamber II
E
Aspect Ratio
****
****
****
AR = L/W
F
Displacement/force (µm/pN)
1 cell
chamber I
chamber II
Time (sec)
G
Restoring stiffness (pN/µm)
*
H
Normalized stiffness
Experiment
Simulation
κ
I
1 cell
Vorticity [1/s]
J
Chamber
Vorticity [1/s]
K
Vortex radius [µm]
**
1 cell
chamber

Figure 4. Cell shape anisotropy enhances the viscoelastic resistance of bulk cytoplasm on mitotic spindles. **(A)** Schemes representing experiments designed to change cell shapes by forcing zygotes in chambers of different geometries. (**B-C)** Time-lapses of metaphase spindles in cells shaped in chamber I (B) and chamber II (C) with magnetic beads bound to one spindle pole, displaced by magnetic forces applied parallel to the spindle axis from the presence of a magnet tip (red line), and recoiling upon force cessation. Dotted lines correspond to the initial centered position of the spindle and arrowheads indicate the positions of chromosomes. **(D-E)** Cell size and aspect ratio quantified as indicated in the inset for cells in control and in chambers (n=10, 8 and 10 cells respectively). **(F)** Time evolution of the displacement normalized by applied magnetic force of metaphase spindles at 1-cell stage in control, in chamber I and in chamber II (n=10, 8 and 10 cells respectively). Error bars are represented as shades in these curves and correspond to +/- S.D/2. **(G)** Restoring stiffness of mitotic spindles for the same cells and conditions as in F (n=10, 8 and 10 cells respectively). Error bars correspond to +/- SEM. **(H)** Restoring stiffness normalized by the 1-cell value in indicated conditions for experimental data vs simulations. **(I-J)** Experimental heatmaps of cytoplasm streamlines averaged on a duration of 50 s for spindles pulled at 1-cell stage in spherical control cells (I) and in cells deformed in a chamber (J). Streamlines are superimposed onto a color map of local flow vorticities, ω. **(K)** Quantification of flow vortex radius for normal cells and cells deformed in chambers (n=8 and 5 cells respectively). Results were compared by using a two-tailed Mann–Whitney test. The corresponding P-values are indicated in the plot. Scale bars, 20 µm.